Bull. Astr. Soc. India (2007) **35**, 339–357

Low-resolution spectroscopy of high Galactic latitude objects: A search for CH stars

Aruna Goswami[1*], P. Bama[2], N. S. Shantikumar[2] and Deepthi Devassy[3†]
[1] *Indian Institute of Astrophysics, Koramangala, Bangalore 560 034, India*
[2] *CREST Campus, Indian Institute of Astrophysics, Hosakote, India*
[3] *Department of Physics, University of Calicut, Calicut, Kerala, India*

Received 22 June 2007; accepted 14 August 2007

Abstract. Properties of CH stars like iron deficiency and enrichment of carbon and heavy elements can provide valuable inputs to our understanding of nucleosynthesis. In particular, these parameters provide strong observational constraints for theoretical studies of nucleosynthesis of heavy elements at low-metallicity. Accurate identification and spectroscopic characterization of CH stars are therefore very essential. We have undertaken a programme with a prime objective to search for these objects in a mixed sample of carbon stars taken from Hamburg/ESO survey. The spectra of the objects were obtained using OMR at VBO, Kavalur and HFOSC at HCT, IAO, Hanle, during 2005 and 2006. Here, we report a detection of twenty-one CH stars from a sample of sixty objects based on low-resolution spectral analysis. Estimated effective temperatures, $^{12}C/^{13}C$ isotopic ratios, and their location in the two colour J-H vs H-K plot support their identification with the class of CH stars. Detection of these potential CH star candidates and their spectral description is the main theme of this paper.

Keywords : stars: CH stars – variable: carbon – stars: spectral characteristics – stars: AGB – stars: population II

*e-mail: aruna@iiap.res.in
†IIA's Summer Project Program student, 2006

1. Introduction

Over the past few decades, surveys on stellar populations have led to the discovery of different types of stars that include numerous metal-poor objects (Beers, Preston & Shectman 1992; Beers 1999; Christlieb 2003). A significant fraction ($\sim$ 20%) of these metal-poor stars (with metallicity [Fe/H] $\leq$ -2) are found to be carbon-enhanced Metal-Poor objects (Lucatello et al. 2005). Carbon stars, that have carbon rich atmosphere (C/O $\geq$1) make-up an important subgroup of stars on AGB. Compared to the normal oxygen-rich stars carbon stars having same mass, are brighter by about one bolometric magnitude and hence the use of C-stars have been largely in practice to probe the kinematics and dynamics of the Galaxy and of external systems (Green et al. 1992, 1994). More recently, chemical composition studies of metal-poor C-stars have demonstrated that significant insight on the neutron-capture processes taking place in the early Galaxy can be derived from these objects (Norris et al. 1997a 1997b, 2002; Bonifacio et al. 1998; Hill et al. 2000; Aoki et al. 2002; Goswami et al. 2006; Aoki et al. 2007). Among them the class of Population II carbon stars, called CH stars, that are characterized by strong G-band of CH and $s-$process elements play significant roles in probing the impact of $s-$process mechanisms in early GCE. Careful abundance analysis of such stars can provide observational constraints for theoretical modelling of $s-$process nucleosynthesis at very low-metallicity revealing the time of influence of this process on early Galactic Chemical Evolution (GCE). However, literature survey shows that not many CH stars have been studied in detail. The main difficulty lies in distinguishing these objects from other carbon stars such as Pop I C-R and C-N stars. Dwarf carbon stars are also very difficult to distinguish from C giants as they exhibit remarkably similar spectra with those of C giants.

Different types of carbon stars have different astrophysical implications and it is important to distinguish them from one another to understand the astrophysical implications of each individual class of stellar population. Due to the many important roles played by CH stars in our understanding of formation and evolution of heavy elements in low-mass, low-metallicity stars as well as in our understanding of early Galactic chemical evolution, we have undertaken to identify the CH stars as well as different types of stellar objects in a selected sample of high Galactic latitude field stars. Using spectral classification criteria presented in Goswami (2005) we have classified the stars based on low resolution spectral analysis. The analysis led to the detection of twenty-one potential CH star candidates. This set of objects will make important targets for subsequent chemical composition studies based on high resolution spectroscopy.

Selection of the programme stars is outlined in Section 2. Observations and data reductions are described in Section 3. In Section 4 we briefly discuss the main features and spectral characteristics of C-stars. Description of the programme stars spectra and results are drawn in Section 5. Concluding remarks are presented in Section 6.

2. Selection of programme stars

Programme stars are primarily chosen from Hamburg/ESO survey of Christlieb et al. (2001). This work presented a sample of 403 stars as Faint High Latitude Carbon (FHLC) stars. The identification of these objects as FHLC stars was based on a measure of line indices - i.e. ratios of the mean photographic densities in the carbon molecular absorption features and the continuum bandpasses. They primarily considered strong C_2 and CN molecular bands shortward of 5200 Å and CH bands were not considered. We have undertaken to search for CH stars in this sample. In an earlier work Goswami (2005) reported spectral classification of ninety-one objects. Here we report another set of sixty objects, listed in Table 1, observed during 2005 and 2006.

3. Observation and data reduction

Observations have been carried out with the 2m Himalayan Chandra Telescope (HCT) at the Indian Astronomical Observatory (IAO), Mt. Saraswati, Digpa-ratsa Ri, Hanle during 2005 - 2006. Spectra of a number of carbon stars such as HD 182040, HD 26, HD 5223, HD 209621, Z PSc, V460 Cyg and RV Sct are also taken for a comparison. The spectrograph used is the Himalayan Faint Object Spectrograph Camera (HFOSC) attached to the Himalayan Chandra Telescope (HCT). HFOSC is an optical imager cum spectrograph for conducting low and medium resolution grism spectroscopy (http://www.iiap.ernet.in/iao/iao.html). The grism and the camera combination used for observations provided a spectral resolution of $\sim 1330(\lambda/\delta\lambda)$; the observed bandpass is from about 3800 to 6800 Å. Spectra for a number of objects were also acquired on Dec 14 & 15, 2006 using OMR spectrograph at the cassegrain focus of the 2.3 m Vainu Bappu Telescope (VBT) at Kavalur. With a 600 lmm^{-1} grating, we got a dispersion of 2.6 Å per pixel. The spectra of these objects cover a wavelength range 4000 - 6100 Å, at a resolution of ~ 1000.

Observations of Th-Ar hollow cathod lamp taken immediately before and after the stellar exposures provided the wavelength calibration. The CCD data were reduced using the IRAF software spectroscopic reduction packages. For each object two spectra were taken each of 15 minutes exposures, the two spectra were combined to increase the signal-to-noise ratio.

4. Spectral characteristics of carbon stars

We briefly discuss here the main characteristics that place carbon stars into different groups. More detailed discussions on the classification of carbon stars can be found in literature (i.e. Wallerstein (1998) and references therein; Goswami (2005)).

Table 1. HE stars observed during 2005 and 2006.

Star No.	RA(2000)[a]	DEC(2000)[a]	l	b	B_J^a	V^a	B-V[a]	U-B[a]	J	H	K	Dt of Obs
HE 0038-0314	00 40 34.6	-02 58 22	116.33	-65.71	15.70	14.4	1.39	1.00	12.833	12.334	12.209	29.01.05
HE 0038-0024	00 40 48.2	-00 08 05	117.09	-62.89	16.26	14.4	1.86	1.67	12.433	11.768	11.573	22.10.05
HE 0114-1129	01 16 40.3	-11 13 14	144.59	-72.02	15.95	14.3	1.65	1.25	12.765	12.216	12.048	23.10.05
HE 0150-2038	01 53 10.9	-20 24 04	190.75	-74.37	15.95	14.2	1.75	1.55	12.367	11.822	11.630	23.10.05
HE 0206-1916	02 09 19.6	-19 01 56	192.69	-70.38	15.07	13.9	1.17	0.63	12.243	11.765	11.660	23.10.05
HE 0219-1739	02 21 41.4	-17 25 37	192.66	-67.03	15.85	14.1	1.75	1.51	12.537	11.884	11.754	22.10.05
HE 0319-0215	03 21 46.3	-02 04 34	184.58	-46.17	15.03	13.6	1.43	1.01	11.785	11.218	11.063	22.10.05
HE 0400-2030	04 02 14.8	-20 21 53	214.75	-46.07	14.80	13.9	0.90	0.44	12.494	12.064	11.975	23.10.05
HE 0430-1609	04 32 50.6	-16 03 38	212.72	-37.76	14.10	13.1	1.38	0.96	11.390	10.885	10.739	18.02.06
HE 0435-2034	04 37 42.1	-20 28 38	218.48	-38.24	14.17	13.0	1.17	1.10	11.223	10.736	10.576	23.10.05
HE 0439-1139	04 41 24.9	-11 33 26	208.66	-34.05	13.4x				10.065	9.417	9.265	23.10.05
HE 0451-2109	04 53 50.2	-21 04 33	220.72	-34.87	13.47	12.2	1.27	1.34	10.141	9.564	9.428	23.10.05
HE 0503-2009	05 06 02.9	-20 05 58	220.77	-31.85	14.30	13.1	1.20	1.08	11.148	10.623	10.498	23.10.05
HE 0513-2008	05 15 14.9	-20 04 59	221.62	-29.81	13.2x				9.398	8.810	8.677	18.02.06
HE 0932-0341	09 35 10.2	-03 54 33	238.38	+33.41	15.13	13.9	1.23	1.02	12.295	11.807	11.708	29.03.05
HE 0939-0725	09 42 11.9	-07 39 06	243.19	+32.50	14.00	13.1	1.20	1.13				18.02.06
HE 0945-0813	09 48 18.7	-08 27 40	245.08	+33.15	16.20	15.3	1.22	1.11	13.531	13.026	12.903	18.02.06
HE 1011-0942	10 14 25.0	-09 57 54	251.77	+36.86	15.85	14.2	1.65	1.76	11.209	10.432	10.125	30.03.05
HE 1018-0218	10 20 43.2	-02 33 47	246.18	+43.10					9.983	9.433	9.308	30.03.05
HE 1019-1136	10 22 14.7	-11 51 39	255.14	+36.81	15.74	13.9	1.84	2.29	10.005	9.031	8.488	29.03.05
HE 1023-1504	10 25 55.5	-15 19 18	258.78	+34.79	16.26	14.4	1.86	1.56	12.323	11.609	11.419	30.03.05
HE 1030-1518	10 33 10.0	-15 33 51	260.62	+35.71	13.3x				10.375	9.801	9.657	18.02.06
HE 1033-2030	10 35 25.1	-20 45 43	264.92	+31.89	13.80	11.9	1.46	1.38	9.833	9.223	9.079	19.02.06
HE 1051-0518	10 54 28.8	-05 34 21	257.71	+46.77	14.68	13.2	1.48	1.26	11.351	10.781	10.625	30.03.05
HE 1053+0053	10 55 51.1	+00 37 22	251.80	+51.64	14.99	14.2	0.79	0.73	12.541	12.033	11.956	29.03.05
HE 1058-2228	11 01 21.8	-22 44 30	272.21	+33.48	14.20	13.5	1.06	0.97	12.040	11.547	11.390	19.02.06
HE 1104-1442	11 06 30.3	-14 58 56	268.60	+40.79	15.01	13.7	1.31	1.16	12.217	11.568	11.470	31.03.05
HE 1145-1118	11 47 37.2	-11 35 27	279.05	+48.30	14.60	12.8	0.92	0.92	11.890	11.525	11.390	18.02.06
HE 1152-0430	11 54 41.9	-04 47 05	277.55	+55.27	15.10	14.0	1.41	1.31	11.618	10.970	10.773	19.02.06
HE 1152-0355	11 55 06.1	-04 12 24	277.32	+55.84	12.3x				9.339	8.665	8.429	29.01.05

[a] From Christlieb et al. (2001)

Table 1. Continued.

Star No.	RA(2000)[a]	DEC(2000)[a]	l	b	B_J^a	V[a]	B-V[a]	U-B[a]	J	H	K	Dt of Obs
HE 1205-1444	12 08 29.6	-15 01 13	287.76	+46.58	15.19	14.0	1.19	1.48	12.120	11.575	11.422	31.03.05
HE 1220-1241	12 23 34.4	-12 58 24	292.48	+49.33	13.54	12.4	1.14	1.15	11.207	10.683	10.543	30.03.05
HE 1230-0230	12 33 26.4	-02 47 08	293.98	+59.77	14.07	12.7	1.37	1.43	10.094	9.421	9.259	29.03.05
HE 1238-1152	12 41 25.0	-12 09 11	299.07	+50.64	15.09	13.8	1.29	1.13	12.221	11.672	11.526	30.03.05
HE 1245-2000	12 48 12.3	-20 16 30	301.90	+42.59					10.127	9.546	9.379	31.03.05
HE 1250-1155	12 53 32.9	-12 12 16	303.75	+50.66	14.00	13.2	1.16	1.16	10.847	10.300	10.144	18.02.06
HE 1305+0007	13 08 03.8	-00 08 48	311.94	+62.43	13.98				10.247	9.753	9.600	29.01.05
HE 1305+0132	13 08 17.8	+01 16 49	312.52	+63.84	13.80	12.8	1.35	1.25	10.621	9.994	9.814	17.03.05
HE 1328-0404	13 31 11.6	-04 19 36	321.41	+57.11	14.6	13.5	1.10	0.94	11.599	11.071	10.930	31.03.05
HE 1331-0247	13 34 32.0	-03 02 30	323.61	+58.09	14.32	13.0	1.32	1.31	10.998	10.394	10.240	30.03.05
HE 1339-0700	13 42 26.8	-07 15 23	424.51	+53.46	15.44	13.7	1.74	1.82	10.520	9.617	9.238	30.03.05
HE 1354-0242	13 56 56.6	-02 57 32	333.18	+56.02	13.59	12.2	1.39	1.39	10.442	9.898	9.756	29.03.05
HE 1404-0755	14 06 44.9	-08 09 23	332.92	+50.28	13.5x				10.877	10.382	10.223	31.03.05
HE 1410+0213	14 13 06.5	+01 59 21	344.28	+58.15	13.90	13.2	1.09	0.68	11.563	11.053	10.968	19.02.06
HE 1418+0150	14 21 01.2	+01 37 18	346.80	+56.66	14.20				9.988	9.356	9.127	19.02.06
HE 1429-1411	14 32 40.6	-14 25 06	336.63	+41.73	13.09	11.1	1.99	1.89	7.622	6.721	6.346	29.01.05
HE 1443-0503	14 46 30.2	-05 16 21	347.90	+47.30	14.25	13.1	1.15	0.94	11.257	10.728	10.572	30.03.05
HE 1522-0503	15 24 42.4	-05 14 29	357.61	+40.82	15.22	14.3	0.92	0.87	12.472	11.990	11.922	31.03.05
HE 2153-2225	21 56 34.3	-22 11 25	30.16	-50.16	14.91	13.5	1.41	1.15	11.446	10.847	10.764	26.07.05
HE 2153-2323	21 56 37.6	-23 09 25			16.10	14.5	1.60	1.44	12.526	11.916	11.741	26.07.05
HE 2200-1652	22 03 19.7	-16 37 35	39.15	-49.81	12.16	11.17			9.562	9.283	8.961	26.07.05
HE 2201-0345	22 03 57.5	-03 30 54	56.05	-43.59	15.36	14.1	1.26	0.53	12.378	11.886	11.773	22.10.05
HE 2205-1033	22 08 29.2	-10 18 37	48.64	-48.17	12.8x				9.732	9.178	8.980	23.10.05
HE 2224-1758	22 27 00.6	-17 43 27	41.04	-55.46	13.81	12.5	1.31	1.31	10.494	9.963	9.839	26.07.05
HE 2225-1401	22 28 10.7	-13 46 23	47.46	-54.05	17.22	14.5	2.72	2.36	11.870	10.748	9.896	26.07.05
HE 2234-1017	22 37 25.4	-10 02 19	54.90	-54.12	15.64	14.2	1.44	1.43	12.420	11.913	11.753	22.10.05
HE 2329-0716	23 31 54.7	-06 59 31	76.16	-62.40	15.75	14.4	1.35	1.04	12.744	12.272	12.163	22.10.05
HE 2339-0837	23 41 59.9	-08 21 19	78.51	-65.05	14.90	14.0	1.32		12.632	12.107	12.026	23.10.05

[a] From Christlieb et al. (2001)

One of the primary objectives of spectral classification is to reduce the number of stars to be analyzed to a tractable number of prototype objects of different classes, such that these classes correlate with one or more physical parameters such as luminosity and temperature. With the consideration of only these two parameters it is difficult to devise such a classification scheme for carbon stars as they exhibit abundance anomalies that cannot be explained on the basis of observed temperature and luminosity.

Assigning stars to 'morphological groups' is largely in practice in modern classification schemes. Carbon stars are primarily classified based on the strength of carbon molecular bands. Morgan-Keenan system for carbon star classification (Keenan 1993) divided carbon stars into C-R, C-N and C-H sequence, with subclasses running to C-R6, C-N6 and C-H6 according to temperature criteria. In the old R-N system, CH stars that were classified as R-peculiar are put is a separate class in the new system.

The C-N stars have stronger molecular bands and lower surface temperatures than those of C-R stars. C-N stars exhibit strong depression of light in the violet part of the spectrum. The cause of rapidly weakening continuum below about 4500Å is not fully established yet, but believed to be due to scattering by particulate matter. Oxygen-rich stars of similar effective temperature do not show such weakening. These stars are easily detectable from their characteristic infrared colours. The majority of C-N stars show ratios of $^{12}C/^{13}C$ more than 30, ranging nearly to 100 while in C-R stars this ratio ranges from 4 to 9 (Lambert et al. 1986).

The characteristic behaviour of s-process elements in C-stars is another useful indicator of spectral type. C-R as well as CH stars have warmer temperatures and blue/violet light is accessible to observation and atmospheric analysis. The s-process elemental abundances are nearly solar in C-R stars (Dominy 1984) whereas CH stars show significantly enhanced abundances of the s-process elements relative to iron (Lambert et al. 1986; Green & Margon 1994). However, at low dispersion the narrow lines are difficult to estimate and essentially do not provide with a strong clue to distinguish C-R stars from CH stars.

CH stars, characterized by strong G-bands of CH, form a group of warm stars of equivalent spectral types G and K normal giants but show weaker metallic lines. In general, CH stars are high velocity objects, large radial velocities indicate they belong to the halo population of the Galaxy (McClure 1983, 1984; McClure & Woodsworth 1990).

As many C-R stars also show quite strong CH bands, the strength and shape of the secondary P-branch head near 4342 Å is used as a more useful indicator to distinguish them. This is a well-defined feature in CH stars spectra in contrast to its appearance in C-R stars spectra. Another important feature is the strength of Ca I at 4226 Å which in case of CH stars is weakened by the overlying faint bands of the CH band systems. In C-R stars this feature is quite strong with band depths deeper than the depth of CN molecular

band around 4215 Å. Strong C-molecular bands but weak CH bands characterizes the class of hydrogen deficient carbon stars.

Another important feature is the strength of the Merrill-Sanford (M-S) bands usually ascribed to SiC_2, that appear in the wavelength region 4900–4977Å. Whenever present these bands appear very strongly in the spectra, with a few exceptions, that show intermediate strength. In general, stars with low $^{12}C/^{13}C$ ratios show strong M-S bands, while stars with weak bands show high $^{12}C/^{13}C$ ratios. WZ Cas, V Aql & U Cam are a few exceptions which have low ^{13}C but strong M-S bands (Barnbaum et al. 1996). SiC_2 being a triatomic molecule, M-S bands are expected to be the strongest in the coolest stars. SiC_2 and C_3 have similar molecular structures and in many C stars C_3 molecule is believed to be the cause of ultraviolet depression (Lambert et al. 1986). M-S bands appear most often in C-J stars, although they are found in some warmer C-N stars. These bands are not known to be present in CH stars.

5. Results and discussions

The spectra of the objects are examined based on the spectral characteristics oulined in the previous section. In summary, the spectra are examined in terms of the following spectral characteristics.

1. The strength (band depth) of CH bands around 4300 Å.
2. Prominance of secondary P-branch head near 4342 Å.
3. Strength/weakness of Ca I feature at 4226 Å.
4. Isotopic band depths of C_2 and CN, in particular the Swan bands of $^{12}C^{13}C$ and $^{13}C^{13}C$ near 4700 Å.
5. Strength of other C_2 bands in the 6000 -6200 Å region.
6. ^{13}CN band near 6360 Å and other CN bands across the wavelength range.
7. Presence/absence of Merrill-Sandford bands around 4900 - 4977Å region.
8. Strength of Ba II features at 4554 Å and 6496 Å.

To establish the membership of a star in a particular group we have conducted a differential analysis of the program stars spectra with the spectra of carbon stars available in the low resolution spectral atlas of carbon stars of Barnbaum et al. (1996). We have also obtained spectra for some objects from this Atlas, whenever possible, to compare the program stars and the comparison stars spectra at the same resolution.

Spectral analysis shows that out of sixty high Galactic latitude objects analysed, forty of them show strong C_2 molecular bands in their spectra. There are twenty objects which do not show prominent C_2 molecular bands in their spectra but show weak but detectable CH and CN bands. Of the forty stars that show strong carbon molecular bands

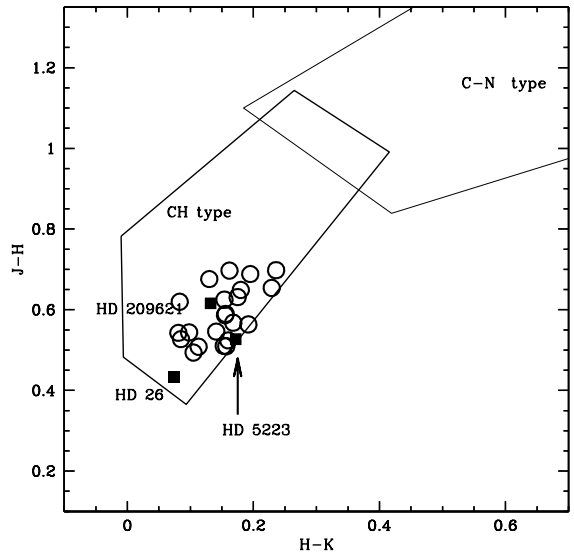

Figure 1. A two colour J-H versus H-K diagram of the stars listed in Table 2. The candidate CH stars are represented by open circles. The two boxes superimposed in the figure illustrate the loci of separate carbon-star types and are taken from Totten et al. (2000). The location of the comparison stars are labeled and marked with solid squares.

twenty-one of them show spectral characteristics of CH stars. These potential CH star candidates are listed in Table 2. In the following we discuss the spectral characteristics of the candidate CH stars.

Location in the two-colour (J-H) vs (H-K) diagram
The stars listed in Table 2 are plotted on a two-colour (J-H) vs (H-K) diagram (Fig. 1) taking 2MASS JHK measurements of the HE stars from on-line[1]. The thick box on the lower left represents the location of CH stars and the thin box on the upper right represents the location of C-N stars (Totten et al. 2000). It is interesting to note that, all the stars listed in Table 2 fall well within the CH box and do not show any anomalies. This supports our identification of these objects as CH stars based on spectral analysis. Location of three well known CH stars HD 26, HD 5223 and HD 209621 used in this study as comparison stars are also shown in the figure.

Effective temperatures of the candidate CH stars
Using temperature calibrations derived by Alonso et al. (1994, 1996, 1998) we have derived the effective temperature of the objects listed in Table 3. The calibrations relate $T_{\rm eff}$ with Stromgren indices as well as [Fe/H] and colours (B-V), (V-K), (J-H) and

[1](http://iras.ipac.caltech.edu/)

Table 2. Potential CH star candidates.

Star No.	RA(2000)[a]	DEC(2000)[a]	l	b	B_J^a	V^a	B-V[a]	U-B[a]	J	H	K	Dt of Obs
HE 0038-0024	00 40 48.2	-00 08 05	117.09	-62.89	16.26	14.4	1.86	1.67	12.433	11.768	11.573	22.10.05
HE 0114-1129	01 16 40.3	-11 13 14	144.59	-72.02	15.95	14.3	1.65	1.25	12.765	12.216	12.048	23.10.05
HE 0150-2038	01 53 10.9	-20 24 04	190.75	-74.37	15.95	14.2	1.75	1.55	12.367	11.822	11.630	23.10.05
HE 0206-1916	02 09 19.6	-19 01 56	192.69	-70.38	15.07	13.9	1.17	0.63	12.243	11.765	11.660	23.10.05
HE 0219-1739	02 21 41.4	-17 25 37	192.66	-67.03	15.85	14.1	1.75	1.51	12.537	11.884	11.754	22.10.05
HE 0319-0215	03 21 46.3	-02 04 34	184.58	-46.17	15.03	13.6	1.43	1.01	11.785	11.218	11.063	22.10.05
HE 1051-0518	10 54 28.8	-05 34 21	257.71	+46.77	14.68	13.2	1.48	1.26	11.351	10.781	10.625	30.03.05
HE 1058-2228	11 01 21.8	-22 44 30	272.21	+33.48	14.20	13.5	1.06	0.97	12.040	11.547	11.390	19.02.06
HE 1152-0355	11 55 06.1	-04 12 24	277.32	+55.84	13.88	11.4			9.339	8.665	8.429	29.01.05
HE 1230-0230	12 33 26.4	-02 47 08	293.98	+59.77	14.07	12.7	1.37	1.43	10.094	9.421	9.259	29.03.05
HE 1305+0007	13 08 03.8	-00 08 48	311.94	+62.43	13.98	12.2			10.247	9.753	9.600	29.01.05
HE 1305+0132	13 08 17.8	+01 16 49	312.52	+63.84	13.80	12.8	1.35	1.25	10.621	9.994	9.814	17.03.05
HE 1328-0404	13 31 11.6	-04 19 36	321.41	+57.11	14.6	13.5	1.10	0.94	11.599	11.071	10.930	31.03.05
HE 1331-0247	13 34 32.0	-03 02 30	323.61	+58.09	14.32	13.0	1.32	1.31	10.998	10.394	10.240	30.03.05
HE 1410+0213	14 13 06.5	+01 59 21	344.28	+58.15	13.90	13.2	1.09	0.68	11.563	11.053	10.968	19.02.06
HE 1418+0150	14 21 01.2	+01 37 18	346.80	+56.66	13.70				9.988	9.356	9.127	19.02.06
HE 2153-2225	21 56 34.3	-22 11 25	30.16	-50.16	14.91	13.5	1.41	1.15	11.446	10.847	10.764	26.07.05
HE 2153-2323	21 56 37.6	-23 09 25			16.10	14.5	1.60	1.44	12.526	11.916	11.741	26.07.05
HE 2201-0345	22 03 57.5	-03 30 54	56.05	-43.59	15.36	14.1	1.26	0.53	12.378	11.886	11.773	22.10.05
HE 2234-1017	22 37 25.4	-10 02 19	54.90	-54.12	15.64	14.2	1.44	1.43	12.420	11.913	11.753	22.10.05
HE 2339-0837	23 41 59.9	-08 21 19	78.51	-65.05	14.90	14.0	1.32		12.632	12.107	12.026	23.10.05

[a] From Christlieb et al. (2001).

(J-K). The estimated uncertainty in T_{eff} determination is ∼90K (Alonso et al. 1996). Estimation of T_{eff} from T_{eff} versus (J-H) & T_{eff} versus (V-K) relations, involve a metallicity term. We have estimated the effective temperatures at three adopted metallicities shown in parenthesis in Table 3.

As noticed from Table 3, in most of the cases, B-V colour calibration is found to return the lowest temperatures that differ by a few hundred K from those derived using other colour calibrations. In case of normal stars the broad-band B-V colour is often used for the determination of T_{eff}. In case of stars with strong carbon molecular features the colour B-V not only depends on T_{eff} but also depends on the chemical composition and metallicity. Due to the effect of CH molecular absorption in the B band, B-V colour often gives a much lower value than the actual surface temperature of the star.

$^{12}C/^{13}C$ isotopic ratios

$^{12}C/^{13}C$ ratios provide an important probe of stellar evolution. This ratio is widely used as a mixing diagnostics. We have estimated this ratio from molecular band depths using the bands of (1,0) $^{12}C^{12}C$ λ 4737 and (1,0) $^{12}C^{13}C$ λ4744. For a majority of the sample stars, the ratio $^{12}C/^{13}C$ ranges from 3 to 5. This ratio for the well known CH stars HD 26, HD 5223 and HD 209621 are respectively 5.9, 6.1 and 8.8 (Goswami 2005). Since the abundance anomalies observed in CH giants are believed to have originated by the transfer of mass from a now extinct AGB companion, the CH giant's atmosphere should be enhanced in triple α products from the AGB star's interior- primarily ^{12}C. The low carbon isotope ratios imply that the material transferred from the now unseen companion has been mixed into the CN burning region of the CH star or constitutes a minor fraction of the envelope mass of the CH star.

Spectral description of the candidate CH stars

HE 0219-1739, HE 0319-0215, HE 1230-0230, HE 1305+0007, HE 1305+0132, HE 1418+0150, HE 2153-2323:

The sprectra of these stars are shown in Fig. 2. Among this set of objects HE 1305+0007 has the highest temperature as derived from T_{eff} vs (J-K) calibration of Alonso et al. (1996). The spectra are characterized by strong G-band of CH around 4300 Å. The secondary P-branch head near 4342 Å is distinctly seen in all the spectra. Ca I line at 4226 Å is not detectable in any of these spectrum. CN band around 4215 Å is strong and seen in all the spectra with band depths almost equal to those of CH band around 4300 Å. C_2 molecular bands around 4700, 5165 and 5635 Å are three prominent features in the spectra. While the C_2 molecular bands around 4700 Å and 5265 Å are of similar strengths the band at 5635 Å is much weaker than these two features. CN molecular band around 5700 Å is barely detectable in these stars spectra. Features due to H_β, Na D I, Ba II at 6496 Å and H_α are distinctly seen on the spectra. As expected Merrill-Sandford bands are not detected in these spectra.

Table 3. Estimated effective temperatures (T_{eff}) from semi-empirical relations.

Star Names	T_{eff} (J-K)	T_{eff} (J-H)	T_{eff} (V-K)	T_{eff} (B-V)
HE 0038-0024	3885.8	4000.3 (−0.5)	4320.8 (−0.5)	3159.8 (−0.5)
		4032.9 (−1.5)	4225.2 (−1.5)	3044.7 (−1.5)
		4066.3 (−2.5)	4147.3 (−2.5)	2975.7 (−2.5)
HE 0114-1129	4302.7	4431.9 (−0.5)	4833.7 (−0.5)	3414.8 (−0.5)
		4465.4 (−1.5)	4776.4 (−1.5)	3289.2 (−1.5)
		4499.5 (−2.5)	4738.2 (−2.5)	3217.1 (−2.5)
HE 0150-2038	4239.8	4448.1 (−0.5)	4536.2 (−0.5)	3288.6 (−0.5)
		4481.7 (−1.5)	4455.4 (−1.5)	3168.2 (−1.5)
		4515.7 (−2.5)	4392.6 (−2.5)	3097.6 (−2.5)
HE 0206-1916	4770.7	4734.7 (−0.5)	4849.2 (−0.5)	4178.9 (−0.5)
		4768.4 (−1.5)	4793.2 (−1.5)	4021.4 (−1.5)
		4802.5 (−2.5)	4756.4 (−2.5)	3942.7 (−2.5)
HE 0219-1739	4101.0	4041.7 (−0.5)	4740.1 (−0.5)	3288.6 (−0.5)
		4074.5 (−1.5)	4674.9 (−1.5)	3168.2 (−1.5)
		4107.9 (−2.5)	4628.5 (−2.5)	3067.6 (−2.5)
HE 0319-0215	4286.8	4360.1 (−0.5)	4565.6 (−0.5)	3728.3 (−0.5)
		4393.6 (−1.5)	4486.9 (−1.5)	3589.7 (−1.5)
		4427.5 (−2.5)	4426.4 (−2.5)	3514.2 (−2.5)
HE 1051-0518	4274.2	4340.5 (−0.5)	4550.5 (−0.5)	3652.2 (−0.5)
		4373.9 (−1.5)	4450.9 (−1.5)	3519.2 (−1.5)
		4407.9 (−2.5)	4387.9 (−2.5)	3442.1 (−2.5)
HE 1058-2228	4526.1	4667.9 (−0.5)	4982.1 (−0.5)	4403.0 (−0.5)
		4701.7 (−1.5)	4937.8 (−1.5)	4235.9 (−1.5)
		4735.8 (−2.5)	4913.5 (−2.5)	4155.2 (−2.5)
HE 1152−0355	3756	3957.3 (−0.5)	4421.2 (−0.5)	2600.5 (−0.5)
		3989.8 (−1.5)	4333.3 (−1.5)	2507.7 (−1.5)
		4023.0 (−2.5)	4259.3 (−2.5)	2304.4 (−2.5)
HE 1230−0230	3953	4724.7 (−0.5)	3863.8 (−0.5)	3823.6 (−0.5)
		4771.2 (−1.5)	3742.9 (−1.5)	3681.1 (−1.5)
		4818.6 (−2.5)	3639.7 (−2.5)	3639.2 (−2.5)
HE 1305+0007	4536	4651.5 (−0.5)	4495.0 (−0.5)	3683.8 (−0.5)
		4685.2 (−1.5)	4411.2 (−1.5)	3547.1 (−1.5)
		4719.3 (−2.5)	4345.4 (−2.5)	3472.0 (−2.5)

Table 3. Continued.

Star Names	T_{eff} (J-K)	T_{eff} (J-H)	T_{eff} (V-K)	T_{eff} (B-V)
HE 1305+0132	3880.8	4121.5 (−0.5)	4200.4 (−0.5)	3856.5 (−0.5)
		4154.6 (−1.5)	4097.3 (−1.5)	3712.6 (−1.5)
		4188.1 (−2.5)	4011.8 (−2.5)	3635.9 (−2.5)
HE 1328-0404	4460.7	4518.1 (−0.5)	4537.7 (−0.5)	4318.9 (−0.5)
		4551.7 (−1.5)	4457.0 (−1.5)	4155.4 (−1.5)
		4585.8 (−2.5)	4394.4 (−2.5)	4075.1 (−2.5)
HE 1331-0247	4175.4	4218.3 (−0.5)	4376.3 (−0.5)	3906.8 (−0.5)
		4251.6 (−1.5)	4284.3 (−1.5)	3760.8 (−1.5)
		4285.3 (−2.5)	4210.1 (−2.5)	3683.7 (−2.5)
HE 1410+0213	4725.2	4594.2 (−0.5)	4856.9 (−0.5)	4339.6 (−0.5)
		4627.9 (−1.5)	4801.6 (−1.5)	4175.3 (−1.5)
		4662.0 (−2.5)	4765.5 (−2.5)	4094.8 (−2.5)
HE 1418+0150	3883.2	4108.0 (−0.5)		
		4141.0 (−1.5)		
		4174.6 (−2.5)		
HE 2153-2225	4416.9	4237.0 (−0.5)	4397.3 (−0.5)	3759.5 (−0.5)
		4270.3 (−1.5)	4306.7 (−1.5)	3619.7 (−1.5)
		4304.1 (−2.5)	4234.0 (−2.5)	3543.8 (−2.5)
HE 2153-2323	4095.2	4183.7 (−0.5)	4376.5 (−0.5)	3481.5 (−0.5)
		4216.8 (−1.5)	4284.5 (−1.5)	3353.1 (−1.5)
		4250.5 (−2.5)	4210.4 (−2.5)	3280.2 (−2.5)
HE 2201-0345	4687.9	4642.4 (−0.5)	4762.7 (−0.5)	4011.4 (−0.5)
		4706.1 (−1.5)	4699.5 (−1.5)	3861.0 (−1.5)
		4740.2 (−2.5)	4655.0 (−2.5)	3782.9 (−2.5)
HE 2234-1017	4467.5	4607.1 (−0.5)	4647.9 (−0.5)	3712.8 (−0.5)
		4640.7 (−1.5)	4575.6 (−1.5)	3574.9 (−1.5)
		4674.9 (−2.5)	4521.6 (−2.5)	3499.6 (−2.5)
HE 2339-0837	4684.2	4530.6 (−0.5)	5132.9 (−0.5)	3906.8 (−0.5)
		4564.3 (−1.5)	5102.9 (−1.5)	3760.8 (−1.5)
		4598.4 (−2.5)	5093.8 (−2.5)	3683.7 (−2.5)

The numbers inside the parentheses indicate the adopted metallicities [Fe/H].

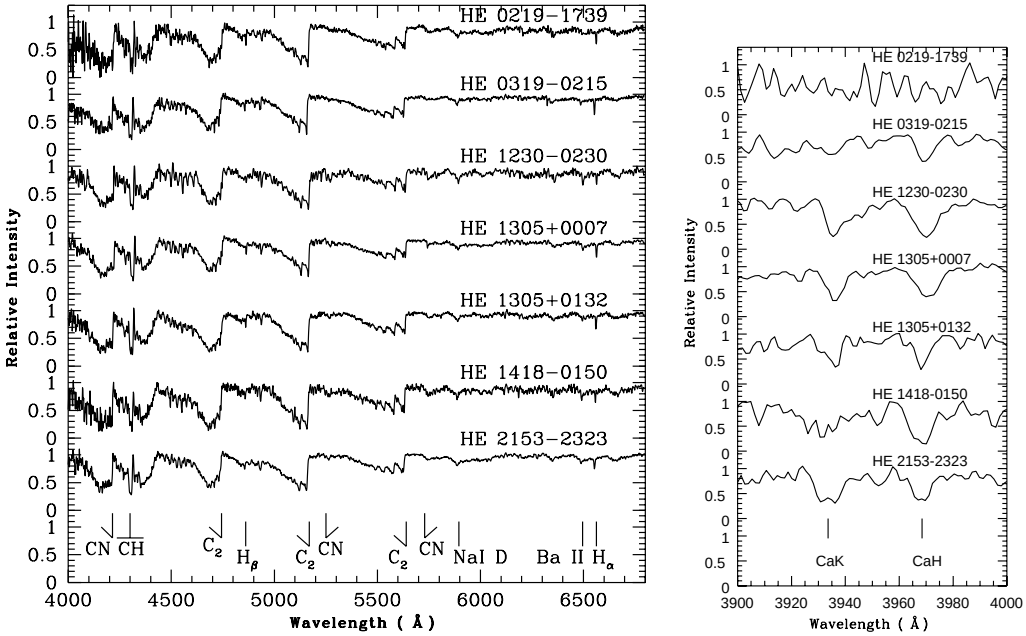

(a) (b)

Figure 2. (**a**) Spectra of candidate CH stars in the wavelength region 4000 - 6800 Å. Locations of the prominent features are marked on the figure. (**b**) The wavelength region 3900 - 4000 Å of the stars presented in Fig. 2(a) with Ca II H and K features marked on the figure.

HE 0114-1129, HE 0150-2038, HE 0206-1916, HE 1152-0355, HE 2201-0345, HE 2234-1017, HE 2339-0837:
The spectra of these objects are shown in Fig. 3. These spectra are very similar to those discussed above except that the C_2 molecular bands around 5635 Å are much weaker in this set of objects. In addition, CN band around 5700 Å that was marginally detected in the above set of spectra is not detectable in this set of objects. Features due to H_β and H_α are prominently seen but Ba II feature at 6496 Å is only marginally detectable. Feature due to Na I D is also distinctly seen. Except in the spectrum of HE 2201+0345, CN band around 4215 Å is strong in all the spectra and of similar band-depths. As in the case of the above set of objects M-S bands are absent in this set of objects. Among this set of objects, HE 0206-1916 is the warmest (4770 K), followed by HE 2201-0345 with 4689 K. HE 1152-0355 is the coolest among the lot with a temperature of 3756 K.

HE 0038-0024, HE 1051-0518, HE 1058-2228, HE 1328-0404, HE 1331-0247, HE 1410+0213, HE 2153-2225:
The spectra of these objects are shown in Fig. 4. As in the previous two sets of objects, the spectra of these stars are also characterized by strong G-band of CH around 4300 Å. C_2

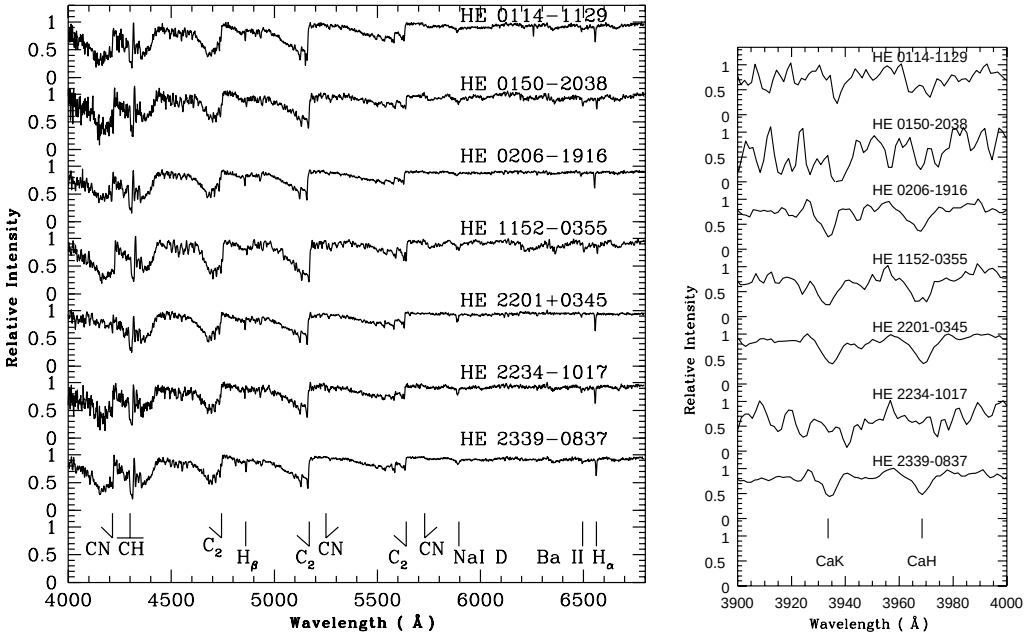

(a) (b)

Figure 3. (**a**) Spectra of candidate CH stars in the wavelength region 4000 - 6800 Å with some prominent features marked on the figure. C_2 band around 5635 Å are shallower than their counterparts in the spectra shown in Fig. 2. (**b**) The wavelength region 3900 - 4000 Å of the stars presented in Fig. 3(a) with Ca II H and K features marked on the figure.

molecular bands although distinctly visible are much weaker in these spectra than those seen in the other two sets of objects discussed above. C_2 molecular band around 5635 Å is marginally detectable except in HE 1058-2228, HE 1328-0404 and HE 1410+0213 where features due to this band seem to be completely absent. In HE 1410+0213, carbon molecular bands around 4700 Å are also weaker than their counterparts in the spectra of other objects. Features due to H_β, H_α and Na D I are distinctly visible. Except in HE 1410+0213 and HE 1058-2228, Ba II features at 6496 Å are also quite distinct in all the spectra. CN molecular bands longward of 5000 Å are not detectable but CN band at 4215 Å is distinctly seen in all the spectra with band depths deeper than those of CH molecular band depths. Among the twenty-one potential CH star candidates, this set of objects include the warmest object HE 1410+0213 with a temperature of 4725 K, and the coolest HE 0038–0024 with a temperature of 3885 K, as derived from $T_{\rm eff}$ – (J-K) calibration (Table 3).

From the estimated low temperature of HE 0038-0024, the star is expected to show strong C_2 molecular bands as against the fact that this star shows very weak C_2 molecular bands, in that, feature due to C_2 molecular band around 5635 Å is only marginally

detectable. This could be an indication of a lower carbon abundance in this star which needs to be confirmed based on high resolution spectroscopic analysis. M-S bands are not detected in any of these star's spectra.

In Figs 2b, 3b and 4b we have shown separately the wavelength region 3900–4000 Å for the stars in Figs 2a, 3a and 4a respectively. An inspection of CaII H and K lines around 3968 Å and 3933.6 Å would help to find which stars are likely to be the most metal-deficient. We however notice that due to the poor quality of the spectra in this region, CaII K line is not detectable in the spectra of stars HE 0219-1739, HE 1305+0132 and HE 1418+0150 (Fig. 2a) and HE 0150-2038, HE 2234-1017, and HE 0114-1129 (Fig 3a). CaII H is also not detectable in the spectra of these stars except in HE 1305+0132 and HE 1418+0150 where this feature could be marginally detected.

Atmospheric parameters derived from high/medium resolution spectroscopy are available in the existing literature for five objects that belong to this list (Table 1). We have summarized in Table 4 the $T_{\rm eff}$, log$g$, [Fe/H], [C/Fe] and [Ba/Fe] for these objects along with their sources. We briefly discuss these objects below.

HE 0206−1916: High resolution (R $\sim$ 50000) spectra of this object was analyzed by Aoki et al. (2007). They derived an effective temperature of 5200 K, log g of 2.7 and metallicity −2.09 for this object. The estimated carbon enhancement was reported as [C/Fe] = +2.10. The $s-$process element barium is enhanced with [Ba/Fe] = +1.97.

HE 0400−2030: Aoki et al. (2007) derived an effective temperature of 5600 K, log g $\sim$ 3.5 and metallicity [Fe/H] = −1.8 for this object from high resolution spectroscopic analysis (R $\sim$ 50000). This object shows a carbon enhancement of [C/Fe] = +1.14. The $s-$process element barium is enhanced with [Ba/Fe] = +1.64. The low resolution spectra of this object acquired by us is characterized by a strong CN molecular band around 4215 Å and a strong G-band of CH around 4310 Å.

HE 1152−0355: From high resolution spectroscopic analysis (R $\sim$ 50000) Goswami et al. (2006) derived an effective temperature of 4000 K, log g $\sim$ 1.0 and a metallicity [Fe/H] = −1.27 for this object. These parameters are derived from excitation balance and ionization equilibrium using Fe I and Fe II lines in their spectra. Carbon and barium were shown to be mildly enhanced with respect to iron with [C/Fe] = +0.58 and [Ba/Fe] = +1.58 respectively.

HE 1305+0007: Goswami et al. (2006) derived the atmospheric parameters $T_{\rm eff}$, log g respectively as 4750 K and 2.0 based on excitation balance and ionization equilibrium using Fe I and Fe II lines in their spectra. A metallicity of [Fe/H] = −2.0 was reported by these authors for this object. From analysis of medium resolution spectra (R $\sim$ 3000) Beers et al. (2007) estimated a temperature of 4560 K, from V-K colour for this object. They derived a metallicity of −2.5 using this temperature estimate. Using a higher temperature 4750 K (from Goswami et al. 2006) they derived a higher metallicity

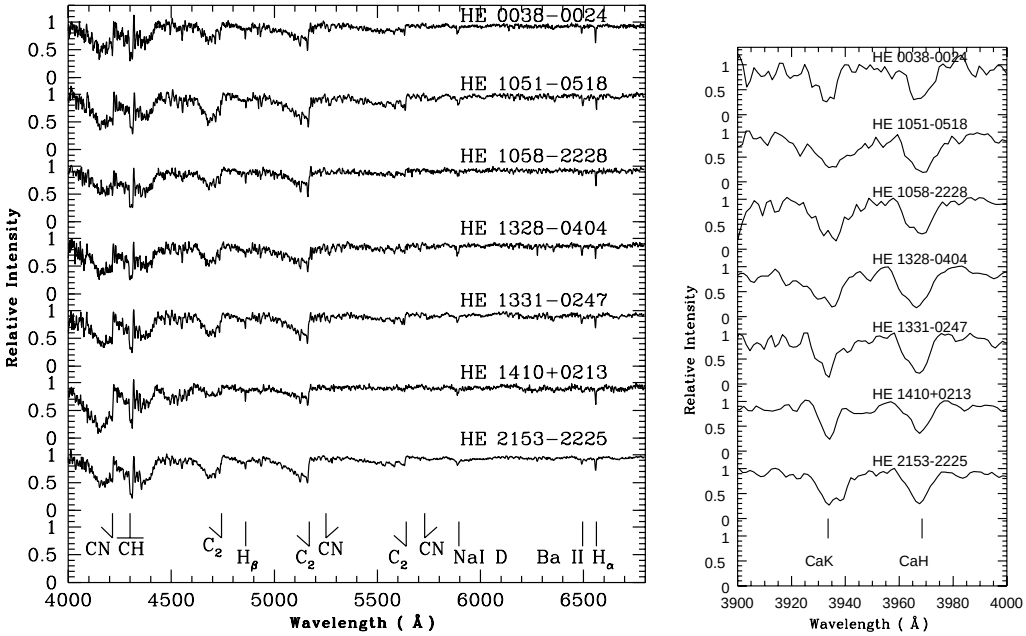

(a) (b)

Figure 4. (**a**) Spectra of candidate CH stars in the wavelength region 4000 - 6800 Å. Some of the prominent features are marked on the figure. Molecular bands that are absent in the first three spectra, in the region longward of 5200 Å, are weakly seen in the lower four spectra. (**b**) The wavelength region 3900 - 4000 Å of the stars presented in Fig 4(a) with Ca II H and K features marked on the figure.

of −2.2 for this star. A carbon enhancement of [C/Fe] = +1.84 and +2.4 and barium enhancement of [Ba/Fe] = +2.32 and +2.9 were reported by Goswami et al. (2006) and Beers et al. (2007) respectively; this difference of 0.6 dex is well within the estimates of the error limits of Beers et al.

HE 1410+0213: Cohen et al. (2006) reported an effective temperature of 5605 K, surface gravity log$g$ = 3.5, and metallicity [Fe/H] = −2.16 for this object. The star exhibits a carbon enhancement of [C/Fe] = +1.73. Unlike the other four objects this object shows almost near-solar abundance for barium with [Ba/Fe] = 0.07 (Cohen et al. 2006).

6. Concluding remarks

The reported findings are based on our on-going observational programmes with HCT and VBT on cool stars. During 2005 and 2006 we have acquired low resolution spectra

Table 4. Objects with known atmospheric parameters.

Star names	T_{eff} K	log g	[Fe/H]	[C/Fe]	[Ba/Fe]	References
HE 0206-1916	5200[a]	2.7	−2.2	+2.10	+1.97	Aoki et al. (2007)
HE 0400-2030	5600[a]	3.5	−1.8	+1.14	+1.64	Aoki et al. (2007)
HE 1152-0355	4000[b]	1.0[b]	−1.27	+0.58	+1.58	Goswami et al. (2006)
HE 1305+0007	4740[b]	2.0[b]	−2.03	+1.84	+2.32	Goswami et al. (2006)
	4560[c]		−2.5	+2.40	+2.9	Beers et al. (2007)
			−2.2[d]			
HE 1410+0213	4980	2.0	−2.16[e]	+1.73	+0.07	Cohen et al. (2006)
	5605	3.5	−2.16	+1.73		Aoki et al. (2006)

a: adopted temperature from broad-band photometry
b: based on excitation balance and ionization equilibrium
c: V-K colour temperature
d: derived using effective temperature from Goswami et al. 2006
e: derived using Fe I lines

for a large number of stars that included about sixty objects from the Hamburg/ESO survey of Chrisltieb et al. (2001). Analysis of these spectra resulted in a detection of twenty-one potential CH star candidates. Their locations in the two colour J-H versus H-K diagram, estimated effective temperatures, and carbon isotopic ratios are in support of their classification with this class of objects. These objects will be taken up for a subsequent high-resolution spectroscopic study for confirmation of these objects with this class of identification and for a detail study of their chemical compositions. Efforts are on to acquire high resolution spectra from the existing 8-10 m class telescopes for some of these objects.

While identification of CN and CJ types are relatively easy, separating C-R stars from CH stars is not so straight forward. C-R stars are believed to be Core Helium Burning (CHeB) counterparts of CH stars in which $s-$process elements are either absent or not detectable (Izzard et al. 2007). C-R stars studied so far are found to be either of solar or slightly sub-solar metallicity (Dominy 1984); in contrast, CH stars cannot be formed above a threshold metallicity, around $Z \sim 0.4Z_{\odot}$ (Abia et al. 2002). Izzard et al. (2007) predicted an early-R/CH ratio $\sim$ 7%, at [Fe/H] = -2.3, a metallicity typical of Galactic halo. This ratio derived considering only CHeB CH stars is likely to get much lower if CH giants and dwarfs are also considered. The two main properties, presence or absence of $s-$process elements and binarity that differentiate early-R stars from CH stars, however can be obtained only through detail abundance studies that require high resolution spectroscopy and from long-term radial velocity monitoring. Due to the faintness of these objects high resolution spectroscopic studies are arduous and time-consuming. As such, the method

described in Goswami (2005) to distinguish a C-R from a CH star proved to be quite useful (Goswami et al. 2006). While in this work we focussed on CH stars, a detail discussion on objects of other spectral types will be available in a sequel (under preparation).

Acknowledgements

This work made use of the SIMBAD astronomical database, operated at CDS, Strasbourg, France, and the NASA ADS, USA. The authors are grateful to the referee Prof. Timothy Beers for his constructive suggestions that improved the paper considerably.

References

Abia, C., Dominguez, I., Gallino, R., Busso, M., Masera, S., Straniero, O., de Laverny, P., Plez, B., & Isern, J., 2002, ApJ, 579, 817
Alonso, A., Arribas, S., & Martinez-Roger, C., 1994 A&AS, 107, 365
Alonso, A., Arribas, S., & Martinez-Roger, C., 1996 A&A, 313, 873
Alonso, A., Arribas, S., & Martinez-Roger, C., 1998 A&AS, 131, 209
Aoki, W., Ryan, S. G., Norris, J. E., Beers, T. C., Ando, H., & Tsangarides, S., 2002, ApJ, 580, 1149
Aoki, W., Beers, T.C., Christlieb, N., Norris, J.E., Ryan, S.G., & Tsangarides, S. 2007, ApJ, 655, 492
Barnbaum, C., Stone, R. P. S., & Keenan, P. 1996, ApJS, 105, 419
Beers, T. C., Preston, G. W., & Shectman, S. A., 1992, AJ, 103, 1987
Beers, T. C., 1999, ASPC, 165, 202
Beers, T. C., Thirupathi, S., Marsteller, B., & Lee YoungSun, 2007, AJ, 133, 1193
Bonifacio, P., Molaro, P., Beers, T. C., & Vladilo, G., 1998, A&A, 332, 672
Christlieb, N., 2003, RvMA, 16, 191
Christlieb, N., Green, P. J., Wisotzki, L., & Reimers, D., 2001, A&A, 375, 366
Cohen, J. G., McWillium, A., Shectman, S., Thompson, I., & Christlieb, N., 2006, AJ, 132, 137
Dominy, J. F. 1984, ApJS, 55, 27
Goswami, A. 2005, MNRAS, 359, 531
Goswami, A., & Prantzos, N., 2000, A&A, 359, 191
Goswami, A., Aoki W., Beers, T. C., Chriestlieb, N., Norris, J. E., Ryan, S. G., & Tsangarides, S., 2006, MNRAS, 372, 343
Green, P. J., Margon, B., Anderson, S. F., & MacConnell, D. J., 1992, ApJ, 400, 659
Green, P. J., Margon, B., Anderson, S. F., & Cook, K. H. 1994, ApJ, 434, 319
Green, P. J., & Margon, B. 1994, ApJ, 423, 723
Hill, V., Barbuy, B., Spite, M., et al., 2000, A&A, 353, 557
Izzard, R. G., Jeffery, C. S., & Lattanzio, J., 2007, A&A (in press) Astro-ph 0705.0894
Keenan Philip, C. 1993, PASP, 105, 905
Lambert, D. L., Gustafsson, B., Eriksson, K., & Hinkle, K-H, 1986, ApJS, 62, 373
Lambert, D. L., Heath, J. E., Lemke, M., & Drake, J., 1996, ApJS, 103, 183
Lucatello, S., Gratton, R. G., Beers, T. C., & Carretta, E., 2005, ApJ 625, L833
McClure, R. D. 1983, ApJ, 268, 264
McClure, R. D. 1984, ApJ, 280, L31

McClure, R. D., & Woodsworth, W., 1990, ApJ, 352, 709
Norris, J. E., Ryan, S. G., & Beers, T. C., 1997a, ApJ, 488, 350
Norris, J. E., Ryan, S. G., & Beers, T. C., 1997b, ApJ, 489, L169
Norris, J. E., Ryan, S. G., Beers, T. C., Aoki, W., & Ando, H., 2002, ApJ, 569, L107
Totten, E. J. et al. 2000, MNRAS, 314, 630
Wallerstein, G., & Knapp, G. 1998, ARA&A, 36, 369